QEXAFS study of the sulfidation of NiMo/Al_2O_3 hydrotreating catalysts

Riccardo Cattaneo, Takafumi Shido and Roel Prins*

Laboratory for Technical Chemistry, Federal Institute of Technology (ETH), CH-8092 Zürich, Switzerland. E-mail: prins@tech.chem.ethz.ch

Quick-scanning extended X-ray absorption fine structure (QEXAFS) spectroscopy was employed to investigate *in situ* the sulfidation of Mo and Ni in γ-Al_2O_3-supported hydrotreating catalysts modified with chelating ligands. Mo *K*-edge QEXAFS enabled the detection of an intermediate product in the sulfidation of Mo. The parameters obtained from the fits of the QEXAFS spectra showed that this product consists of compounds similar to $Mo_2S_{12}^{2-}$ or $Mo_3S_{13}^{2-}$. QEXAFS also demonstrated that the sulfidation of Ni is strongly influenced by the presence of chelating ligands. Classical EXAFS spectra of the sulfided catalysts showed that Ni forms small sulfided clusters, the size of which is influenced by the presence or absence of the chelating agents.

Keywords: QEXAFS; sulfidation; hydrotreating catalysts; nickel–molybdenum/alumina.

1. Introduction

The removal of S, N, O and heavy metals is an indispensable step in the refining of petroleum. This so-called hydrotreating process must be improved because of stricter legislation concerning the S and N content in oil fractions. In order to optimize the reactivity of the CoMo and NiMo hydrotreating catalysts used in the removal of S and N, a better understanding of the processes used to produce these catalysts is necessary. The study reported here deals with one of the fundamental steps in the preparation of hydrotreating catalysts: presulfiding. Presulfiding is carried out before catalysts are used in hydrotreating reactions in order to convert the oxidic catalyst precursor into the final sulfided catalyst.

Presulfiding consists of heating the catalyst precursor to 673 K in the presence of H_2S. Under these conditions and because of the dynamics of the system, the study must be carried out *in situ*. Quick scanning extended X-ray absorption fine structure (QEXAFS) was used to characterize the various steps in the sulfidation of Mo and Ni in γ-Al_2O_3-supported catalysts.

An investigation of the effect of chelating ligands on the sulfidation of Mo as well as of Ni is reported. Such ligands improve the hydrodesulfurization (HDS) activity of the catalysts (van Veen *et al.*, 1987). Our previous work concentrated on the characterization of such modified NiMo/SiO_2 catalysts in the oxidic and sulfided state (Medici & Prins, 1996*a*; Medici & Prins, 1996*b*; Cattaneo *et al.*, 1999, 2000). The aim of this work was to learn more about γ-Al_2O_3-supported materials.

The main goal of this work was to investigate the influence of chelating ligands on the sulfidation temperature of Mo and Ni. An analysis of the data also provided important information about the sulfidation mechanism of Mo and Ni in the absence of chelating agents.

2. Experimental

2.1. *Catalyst preparation*

The catalysts used contained about 7 wt% Mo and 2.5 wt% Ni and were prepared by pore volume co-impregnation of γ-Al_2O_3 (Condea; pore volume: 0.5 $cm^3\ g^{-1}$; specific area: 100 $m^2\ g^{-1}$) with an aqueous solution (pH 9.5) of $(NH_4)_6Mo_7O_{24}.4H_2O$ (Aldrich) and $Ni(NO_3)_2.6H_2O$ (Aldrich) with 25% ammonia in the presence or absence of the chelating ligands nitrilotriacetic acid (NTA) and ethylenediaminetetraacetic acid (EDTA). The support was dried at 393 K for 12 h prior to impregnation. The impregnated powder was dried in air at ambient temperature for 4 h and then dried in an oven at 393 K for 15 h. The other catalysts were not calcined so as to avoid the decomposition of the complexes in the catalyst precursors.

2.2. *XAFS measurements*

The QEXAFS measurements were carried out at the X1 (RÖMO II) beamline at the Hamburger Synchrotronstrahlungslabor (HASYLAB) in Hamburg, Germany (Krolzig *et al.*, 1984; Frahm, 1989; Tröger, 1997). Si (311) and Si (111) crystals were used in the monochromator for the Mo and Ni *K* edges, respectively. The accumulation time was about 0.2 s $step^{-1}$ at the Mo *K* edge and about 0.4 s $step^{-1}$ at the Ni *K* edge. The *k* ranges used for the analysis of the data were 3–17 $Å^{-1}$ for the Mo *K* edge and 3–12 $Å^{-1}$ for the Ni *K* edge. The EXAFS spectra were collected at the Swiss–Norwegian beamline (SNBL, BM01) at the European Synchrotron Radiation Facility (ESRF) in Grenoble, France (Cattaneo *et al.*, 1999). The *k* range used for the analysis of the $\chi(k)$ data was 3–19.5 $Å^{-1}$ for the Mo *K* edge and 3–16 $Å^{-1}$ for the Ni *K* edge.

For both measurements, the catalyst samples were pressed into self-supporting wafers and mounted in an *in situ* EXAFS cell (Kampers *et al.*, 1989). The thickness of the samples was chosen to adjust the edge jump to 1 for the Mo *K* edge and the total absorption to $\mu x = 4$ for the Ni *K* edge (lower Ni concentration).

For the QEXAFS measurements, two spectra of the fresh samples in an He atmosphere were collected. The samples were then sulfided *in situ* during data collection. A stream of 10% H_2S/H_2 flowed through the cell while it was heated to 673 K at a rate of 3 K min^{-1}.

For the classical EXAFS measurements, the samples were cooled to room temperature after they had been sulfided at 673 K for 30 min. Once at room temperature, the H_2S still present in the cell was replaced by He by flushing for 10 min. The cell was then cooled to liquid nitrogen temperature prior to the EXAFS measurement.

The program *XDAP* (version 2.2.2) was used to analyse and fit the data (Vaarkamp *et al.*, 1995). Apart from MoS_2 (experimental references for Mo–S and Mo–Mo were obtained from molybdenite), reference spectra were calculated using the *FEFF7* code (Zabinsky *et al.*, 1995; Ankudinov & Rehr, 1997).

3. Results

3.1. *Mo K-edge QEXAFS*

The QEXAFS spectra measured during the sulfidation of the NiMoEDTA/Al_2O_3 catalyst with a molar ratio of EDTA:Ni = 1 were plotted against the sulfidation temperature (Fig. 1). The spectrum of the fresh catalyst shows Mo–O contributions between 0.8 and 2 Å (phase uncorrected) and an Mo–Mo shell at 3 Å (phase uncorrected). The latter shell suggests the presence of polymolybdates in the catalyst precursor. The nature of the signal at 2.2 Å (phase uncorrected) is not clear and may arise from Mo–support interactions.

The first effect of sulfidation becomes visible in the spectrum measured at 383 K, in which an Mo–S signal appears at a distance of

2 Å (phase uncorrected) from the absorber atom. In the spectrum measured around 413 K, another signal becomes visible at 2.5 Å (phase uncorrected). The same signal has been observed in the spectra of SiO_2-supported NiMo catalysts and was attributed to an Mo–Mo shell present in an intermediate product of the sulfidation of molybdenum (Cattaneo *et al.*, 2000). The Mo–S and Mo–Mo signals grow with increasing sulfidation temperature, until they reach a maximum in the spectrum recorded at 508 K. Thereafter, the two signals decrease in intensity. At around 573 K, the amplitude of the Mo–S signal increases again and a new signal appears at 3 Å (phase uncorrected). The latter signal is an Mo–Mo shell that belongs to MoS_2, the final product of the sulfidation.

Very similar series of spectra were obtained for the sulfidation of Mo for catalysts containing no ligands and for catalysts containing NTA. A first analysis enables us to conclude only that Mo is present as a mixture of MoO_4^{2-} and polymolybdate anions in the catalyst precursors and that the final product of the sulfidation is MoS_2. The nature of the intermediate product, characterized by the signal at 2.5 Å (phase uncorrected), was revealed by fitting the spectra collected at temperatures between 473 and 573 K. The fits showed that the product in this sulfidation interval has an Mo–S distance of 2.5 Å and an Mo–S coordination number higher than 6, usually 6.5 to 7. The second signal was fitted with an Mo–Mo reference; an Mo–Mo distance of 2.79 Å was obtained. Even though the QEXAFS spectra were collected at elevated temperature, it is possible to determine the structure of the intermediate product of the sulfidation. Considering the short Mo–Mo distance, it consists of a species in which Mo has the oxidation state IV or V. A survey of various Mo–S compounds revealed that the intermediate species must be similar to $Mo_2^{V}S_{12}^{2-}$ (Wignacourt *et al.*, 1992) or $Mo_3^{IV}S_{13}^{2-}$ (Müller *et al.*, 1979). The structures of these compounds are depicted in Fig. 2.

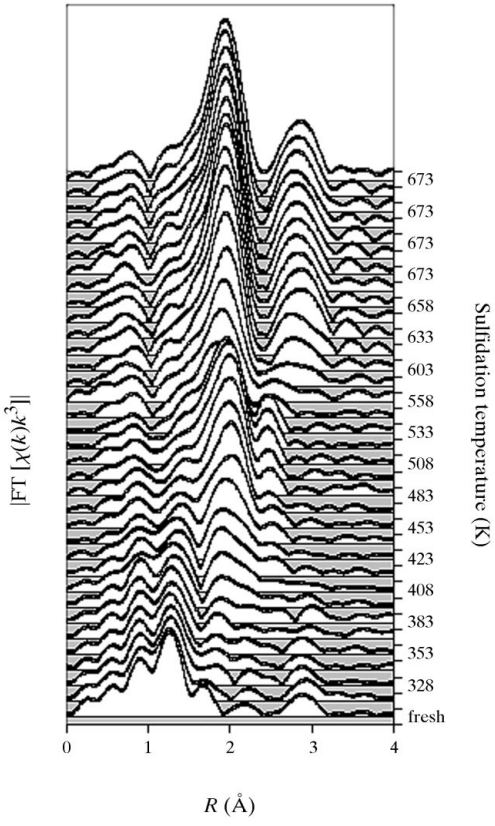

Figure 1
Mo *K*-edge Fourier-transformed spectra obtained from the QEXAFS data collected during the sulfidation of the catalyst NiMoEDTA/Al_2O_3 (molar ratio EDTA:Ni = 1).

3.2. *Ni K-edge QEXAFS*

The QEXAFS technique was also employed to investigate the sulfidation of Ni on alumina-supported catalysts. Fig. 3 shows a sequence of QEXAFS spectra collected during the sulfidation of the dried NiMo/Al_2O_3 catalyst. The signal at 1.6 Å (phase uncorrected) was fitted with an Ni–O shell and a coordination number of 5.4 was obtained, suggesting octahedral coordination. In contrast, the nature of the signal at 2.7 Å (phase uncorrected) could not be established from the QEXAFS data. The extent of sulfidation of Ni can be viewed by monitoring the position of the first signal, which represents the Ni–O shell. This signal moves to longer distances when the oxygen ligands around Ni are replaced by S ligands, because the Ni–S distance is several tenths of an ångstrom longer than the Ni–O distance. A first shift in the shell is seen in the spectrum collected around 388 K and a gradual shift is detected until the spectrum measured at 543 K. The second shell (2.7 Å, phase uncorrected) disappears at 508 K, but a new weak signal appears, at a similar distance, starting from a sulfidation temperature of 558 K. Classical EXAFS is the only way to determine the nature of this signal, which was measured at lower temperatures.

Fig. 4 shows the sulfidation process of Ni, as followed by QEXAFS, for the catalyst containing NTA with a molar ratio of NTA:Ni = 1. The spectrum of the oxidic precursor is very different from that of the catalyst prepared without ligands (Fig. 3). In the presence of NTA, the Ni–C contribution is recognizable around 2.4 Å (phase uncorrected). The shoulder at 2.1 Å (phase uncorrected) is an artefact produced by the interference of the Ni–O and Ni–C shells (Cattaneo *et al.*, 1999). The sulfidation process is also different in comparison with that of the catalyst prepared without ligands. The shift in the first shell is observed from 423 K to 523 K. The Ni–C signal is observed until 548 K.

The comparison of the Ni *K*-edge QEXAFS spectra recorded during the sulfidation of catalysts prepared in the presence and absence of chelating ligands shows that the sulfidation mechanism of Ni is strongly affected by the presence of the chelating ligands. In

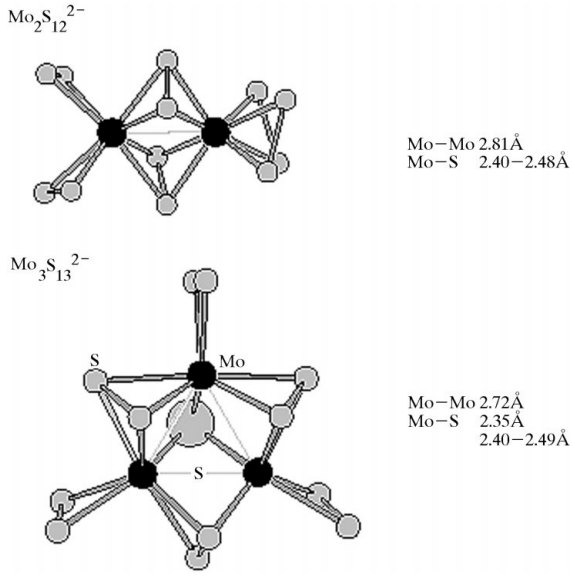

Figure 2
Structure of $Mo_2S_{12}^{2-}$ and $Mo_3S_{13}^{2-}$. The Mo–Mo and Mo–S distances are given.

view of the fact that the Ni–C contribution is still visible at such a high temperature, the ligands probably react with H_2S during the sulfidation. The type of reaction involved in the sulfidation of ligands should be investigated with appropriate techniques, but it is possible to deduce the reaction pathway by studying the structure of Ni in the final sulfided catalysts.

For this purpose, classical EXAFS measurements of the sulfided catalysts were made at liquid-nitrogen temperature. The Ni *K*-edge k^3-weighted $\chi(k)$ and Fourier-transformed data of the sulfided catalyst NiMoNTA/Al_2O_3 with a molar ratio of NTA:Ni = 1 are presented in Fig. 5. As far as the first shell is concerned, there is no doubt that it consists of an Ni–S contribution. The other two shells, on the contrary, were very difficult to fit because they were so close and because of the low amplitude of the signals. The best fit was obtained using Ni–S shells. We obtained convergence for the k^1- as well as the k^3-weighted fits for only this combination of shells. The parameters resulting from the fits of three sulfided catalysts are given in Table 1. The results contrast with previous results reported for similar catalysts supported on carbon (Louwers & Prins, 1992). An Ni *K*-edge *k* range of 3–16 Å^{-1} was used for the analysis of the data. High-quality data were obtained by measuring over long periods and using a relatively high Ni loading. The *k* range of the data used in previous work was generally 3–11 Å^{-1}. The Ni loading in our catalysts was about twice as high as that used by Louwers & Prins (1992). Using the shell combinations proposed by Louwers & Prins (1992), we did not obtain convergence of the fits. This divergence may be caused by the different Ni loadings, which can induce the formation of other Ni species.

Table 1
Structural parameters obtained from the fits of the Ni *K*-edge EXAFS spectra of the alumina-supported catalysts prepared in the absence and presence of NTA.

R = interatomic distance. $\Delta\sigma^2$ = Debye–Waller Factor. ΔE^0 = energy correction.

Catalyst	Shell	Coordination number	*R* (Å)	$\Delta\sigma^2$ (10^3 Å^2]	ΔE^0 (eV)
No ligands	Ni–S	3.4 ± 0.2	2.20 ± 0.01	1.2 ± 0.2	1.4 ± 1.2
	Ni–S	1.2 ± 0.4	2.74 ± 0.1	2.1 ± 0.8	−0.6 ± 4.2
	Ni–S	0.7 ± 0.5	3.06 ± 0.2	−0.2 ± 1.1	−2.7 ± 10.1
NTA:Ni = 1	Ni–S	3.5 ± 0.2	2.19 ± 0.01	1.0 ± 0.9	2.4 ± 1.2
	Ni–S	1.2 ± 0.3	2.74 ± 0.1	3.2 ± 1.7	−0.1 ± 9.1
	Ni–S	0.6 ± 0.5	3.09 ± 0.1	−3.5 ± 0.9	−4.9 ± 12.8
NTA:Ni = 1.5	Ni–S	3.4 ± 0.3	2.20 ± 0.01	1.0 ± 0.8	1.1 ± 1.4
	Ni–S	1.6 ± 0.7	2.74 ± 0.09	4.1 ± 2.1	−0.1 ± 7.7
	Ni–S	0.9 ± 0.5	3.05 ± 0.13	0.2 ± 5.6	0.1 ± 14.7

The obtained parameters for the structure of Ni in the sulfided catalysts show no similarity to inorganic Ni–S compounds such as Ni_3S_2, NiS or NiS_2. In contrast, they do resemble the parameters of the metallorganic trimeric compound bis(dithiobenzoato)nickel(II), the structure of which is depicted in Fig. 6 (Bonamico *et al.*, 1975). In this trimer, two Ni atoms have a quadratic pyramidal geometry, while the central Ni atom possesses an octahedral geometry. The EXAFS spectrum of this compound was simulated by means of *FEFF7*. Fig. 7 shows a comparison of the simulated spectrum and the spectrum of the catalyst NiMoNTA/Al_2O_3 with the molar ratio NTA:Ni = 1. The shift between the measured and simulated $\chi(k)$ functions is due to the fact that the Ni–S distance in the trimeric unit is slightly longer than

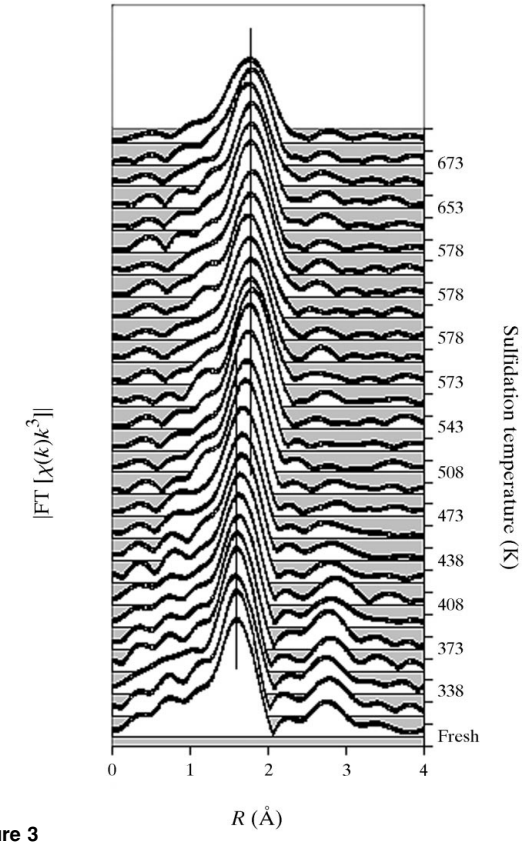

Figure 3
Ni *K*-edge Fourier-transformed spectra obtained from the QEXAFS data collected during the sulfidation of the catalyst NiMo/Al_2O_3 (without ligands).

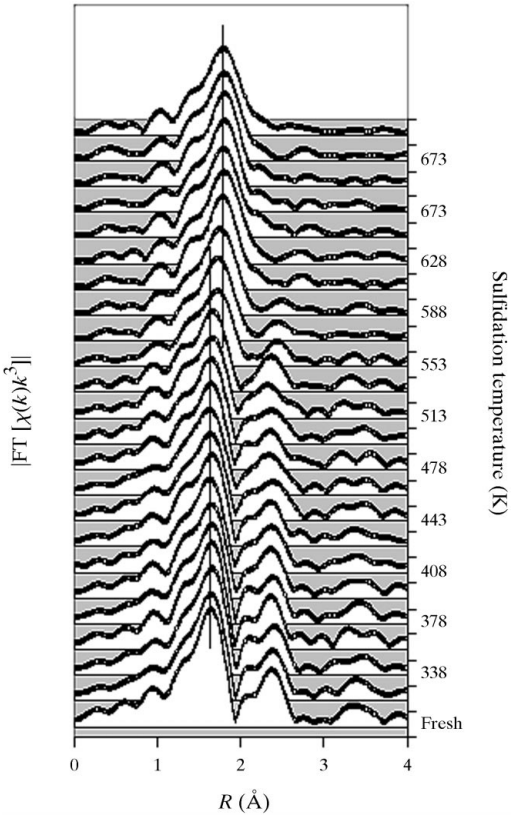

Figure 4
Ni *K*-edge Fourier-transformed spectra obtained from the QEXAFS data collected during the sulfidation of the catalyst NiMoNTA/Al_2O_3 (molar ratio NTA:Ni = 1).

the corresponding distance in our catalyst, which induces a shorter period of sinusoidal oscillation.

The main difference between the Fourier-transformed spectra is the presence of a relatively strong Ni–Ni contribution in the simulated spectrum at 3.4 Å (not phase corrected), which is almost absent in the spectrum of the catalyst. This weak signal in the spectrum of our catalyst may be caused by the overlapping of Ni–Ni contributions with slightly different distances. Moreover, it would be useful to measure classical EXAFS of the sulfided catalysts at liquid-helium temperature in order to check whether or not thermal disorder influences the detection of the Ni–Ni contribution. It should also be noted that the Ni–S coordination number for the second shell is always larger than 0.7 (see Table 1). In the trimeric complex, the corresponding Ni–S coordination number is 0.66, because only two Ni atoms have an S neighbour at 2.78 Å. The high coordination number obtained for our catalysts must, therefore, be due to either the fact that the structure of the clusters is different from the trimeric structure or the fact that the Ni–S contribution is superimposed on another contribution.

Nevertheless, the similarity of the structure of Ni in the sulfided catalysts to the reported trimeric complex suggests that Ni forms small clusters during sulfidation. The chelating ligands play an essential role in the formation of these clusters. Even though it is difficult to deduce the dispersion of Ni from the presented data, it is likely that the chelating agents induce the formation of smaller clusters and consequently a greater dispersion of Ni.

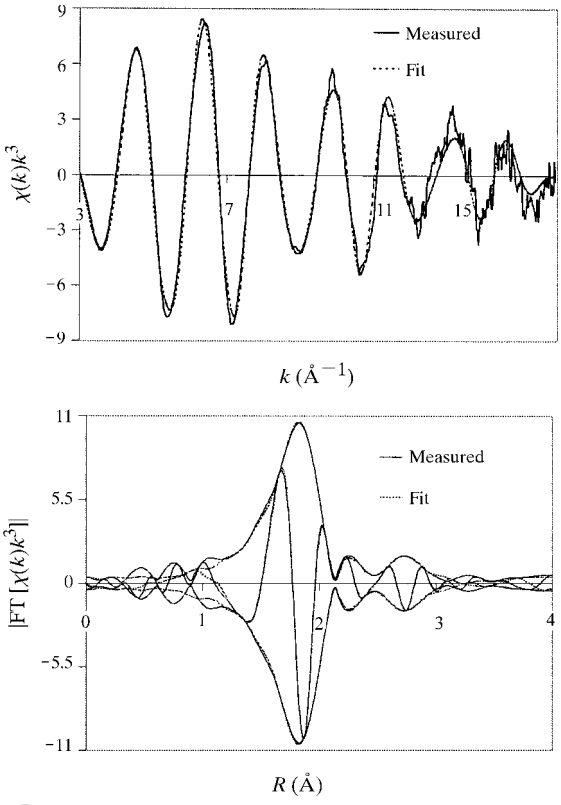

Figure 5
k^3-weighted Ni K-edge $\chi(k)$ (upper panel) and Fourier-transformed (lower panel) spectra of the catalyst NiMoNTA/Al_2O_3 (molar ratio NTA:Ni = 1) sulfided at 673 K for 30 min. The dotted lines indicate the fit obtained with three Ni–S shells.

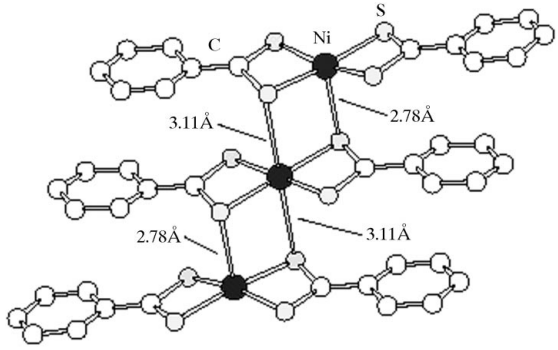

Figure 6
Structure of trimeric bis(dithiobenzoato)nickel(II) (Bonamico *et al.*, 1975).

4. Conclusions

QEXAFS proved to be very important for understanding some of the processes that take place during the sulfidation of supported NiMo hydrotreating catalysts. This technique enabled us to follow the reaction *in situ* and to make a detailed study of the mechanism of sulfidation of Mo and Ni. This technique has limitations: data are collected in a very short period of time, so that the quantitative information that can be extracted from the QEXAFS spectra is

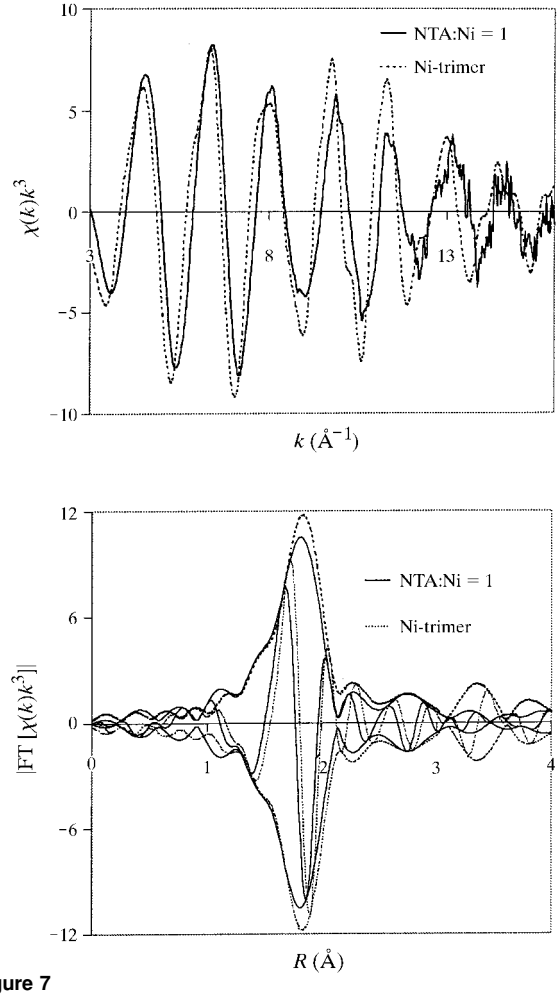

Figure 7
Comparison of the measured spectrum of the catalyst NiMoNTA/Al_2O_3 (molar ratio NTA:Ni = 1) and the simulated spectrum of the trimeric complex: k^3-weighted $\chi(k)$ function (upper panel) and Fourier transformation of the k^3-weighted (k) function (lower panel).

limited. However, this problem can be overcome by combining the quick scanning mode with classical EXAFS.

Experimental assistance from the staff of the RÖMO II station at HASYLAB and the staff of the Swiss–Norwegian beamline at ESRF is gratefully acknowledged. This work was supported by the Swiss National Science Foundation.

References

Ankudinov, A. L. & Rehr, J. J. (1997). *Phys. Rev. B*, **56**, R1712–R1715.
Bonamico, M., Dessy, G., Fares, V. & Scaramuzza, L. (1975). *J. Chem. Soc. Dalton Trans.* pp. 2250–2255.
Cattaneo, R., Shido, T. & Prins, R. (1999). *J. Catal.* **185**, 199–212.
Cattaneo, R., Weber, Th., Shido, T. & Prins, R. (2000). *J. Catal.* **191**, 225–236.
Frahm, R. (1989). *Rev. Sci. Instrum.* **60**, 2515–2518.
Kampers, F. W. H., Maas, T. M. J., van Grondelle, J., Brinkgreve, P. & Koningsberger, D. C. (1989). *Rev. Sci. Instrum.* **60**, 2635–2638.
Krolzig, A., Materlik, G., Swars, M. & Zegenhagen, J. (1984). *Nucl. Instrum. Methods*, **219**, 430–434.
Louwers, S. P. A. & Prins, R. (1992). *J. Catal.* **133**, 94–111.
Medici, L. & Prins, R. (1996*a*). *J. Catal.* **163**, 28–37.
Medici, L. & Prins, R. (1996*b*). *J. Catal.* **163**, 38–49.
Müller, A., Pohl, S., Dartmann, M., Cohen, J. P., Bennett, M. J. & Kirchner, R. M. (1979). *Z. Naturforsch.* **34**, 434–436.
Tröger, L. (1997). *Synchr. Rad. News* **6**, 11–17.
Vaarkamp, M., Linders, J. C. & Koningsberger, D. C. (1995). *Phys. Rev. B*, **209**, 159–160.
Veen, J. A. R. van, Gerkema, E., van der Kraan, A. M. & Knoester, A. (1987). *J. Chem. Soc. Chem. Commun.* **22**, 1684–1986.
Wignacourt, J. P., Drache, M., Swinnea, J. S., Steinfink, H., Lorriaux-Rubbens, A. & Wallart, F. (1992). *Can. J. Appl. Spectrosc.* **37**, 49–54.
Zabinsky, S. I., Rehr, J. J., Ankudinov, A., Albers, R. C. & Eller, M. J. (1995). *J. Phys. Rev. B*, **52**, 2995–3009.